Chinese Chemical Letters 35 (2024) 109343

Contents lists available at ScienceDirect

Chinese Chemical Letters

journal homepage: www.elsevier.com/locate/cclet

A giant Ce-containing poly(tungstobismuthate): Synthesis, structure and catalytic performance for the decontamination of a sulfur mustard simulant

Chen Lian [b], Si-Han Zhao [a], Hai-Lou Li [a,*], Xinhua Cao [a,*]

[a] College of Chemistry and Chemical Engineering, Xinyang Normal University, Xinyang 464000, China
[b] MOE Key Laboratory of Cluster Science, School of Chemistry and Chemical Engineering, Beijing Institute of Technology, Beijing 102488, China

ARTICLE INFO

Article history:
Received 26 October 2023
Revised 14 November 2023
Accepted 29 November 2023
Available online 6 December 2023

Keywords:
Polyoxometalates
Tungstobismuthate
Cluster
Lanthanide
Oxidation

ABSTRACT

A novel Ce-containing poly(tungstobismuthate) $Cs_{18}Na_8H_{20}[Ce_3(H_2O)_{10}W_8Bi_4O_{28}(B\text{-}\alpha\text{-}BiW_9O_{33})_4]_2\cdot 64H_2O$ (**1**) has been synthesized by a facile one-pot self-assembly reaction strategy. Its structural characterization is realized by virtue of single-crystal X-ray diffraction, infrared spectroscopy, powder X-ray diffraction and thermogravimetric analysis. The polyoxoanion of **1** is an octameric architecture consisting of two tetrameric entities $[Ce_3(H_2O)_{10}W_8Bi_4O_{28}(B\text{-}\alpha\text{-}BiW_9O_{33})_4]^{23-}$ linked by two Ce–O–W bonds, and adjacent polyoxoanions are further combined together by means of Ce^{3+} linkers, resulting in an infinite 1D chain architecture. Compound **1** is the currently largest tungstobismuthate, and also represents the first example of lanthanide-encapsulated tungstobismuthate exhibiting an extended structure. Furthermore, compound **1** as a heterogeneous catalyst, exhibits high activity for the oxidative decontamination of a sulfur mustard simulant, 2-chloroethyl ethyl sulfide (CEES) into 2-chloroethyl ethyl sulfoxide (CEESO).

Polyoxometalates (POMs) are a large and rapidly growing kind of anionic metal-oxo clusters with fascinating configurations and an almost unparalleled range of physicochemical properties [1–10]. The adjustability of composition elements, heteroatom types and basic construction unit arrangement patterns gives rise to a large class of POM building blocks featuring structural diversity in shape, size and symmetry [11–15]. More importantly, these POM building blocks are highly negatively charged species characterized by their oxygen-enriched surfaces and show high affinity for transition metal (TM) and/or lanthanide (Ln) ions, so they are widely used as inorganic multidentate ligands to construct novel metal-incorporated POMs with various functionalities [16–23]. As an important branch, Ln-containing POMs (Ln-POMs) have attracted extensive and strong concern [24–27]. The versatile and oxyphilic Ln cations can integrate multiple POM fragments together into huge aggregates or extended structures with unique aesthetic characteristics. Moreover, the combination of POMs and Ln cations within one molecular structure can synergize the advantages of both, thereby enhancing their potential applications, especially in the fields of luminescence, magnetism and materials science [28–30].

Recently, the template effect of pyramidal heteroatoms X (*e.g.*, As^{III}, Sb^{III}, Bi^{III}, Se^{IV}, and Te^{IV}) has emerged as an effective strategy to prepare novel Ln-POMs. In the one-pot reaction system of self-assembled cluster structures, the stereochemical effect of lone-pair orbital electrons at the heteroatom bonded to three oxygen atoms forming XO_3 trigonal pyramid facilitates the *in-situ* assembling into unsaturated POM building blocks that own high active sites to interact with Ln metal centers [31–35]. On the other hand, these pyramidal heteroatoms can also play important bridging roles in condensing Ln cations or/and POM building blocks, which is conductive to fabricating high-nuclear multimers. So far, the wide interest and tremendous efforts in this area have resulted in quite a large number of novel Ln-POMs. Some representative examples of structurally and functionally remarkable compounds include $[Ce_{16}As_{12}(H_2O)_{36}W_{148}O_{524}]^{76-}$ [36], $[\{Eu(H_2O)_2(\alpha\text{-}AsW_9O_{33})\}_6]^{36-}$ [37], $[\{(XO_3)W_{10}O_{34}\}_8\{Ce_8(H_2O)_{20}\}(WO_2)_4(W_4O_{12})]^{48-}$ (X = Se, Te) [38], $[Ce_{10}Te_8W_{88}O_{298}(OH)_{12}(H_2O)_{40}]^{18-}$ [39], $\{[W_2Nd_2(H_2O)_8O_6(OH)_2(Se_2W_{14}O_{52})][W_3Nd_2(H_2O)_6O_7(SeW_9O_{33})_2]_2\}^{20-}$ [40], $[Ce_2W_4O_9(H_2O)_7(SeW_9O_{33})_3]_2^{24-}$ [41], *etc.*

Compared with the rich structural configurations of As/Se/Te-based Ln-POMs mentioned above, the synthesis and exploration of Bi analogues remain less developed probably owing to the relatively high hydrolyzation. Up to now, only a handful of Ln-POMs with Bi as central heteroatoms have been prepared and structurally characterized, as exemplified by three isomorphic tetramers $[(BiW_9O_{33})_4(WO_3)\{Bi_6(\mu_3\text{-}O)_4(\mu_2\text{-}OH)_3\}(Ln_3(H_2O)_6CO_3)]^{22-}$ (Ln =

* Corresponding authors.
E-mail addresses: lhl@xynu.edu.cn (H.-L. Li), caoxhchem@163.com (X. Cao).

https://doi.org/10.1016/j.cclet.2023.109343
1001-8417/

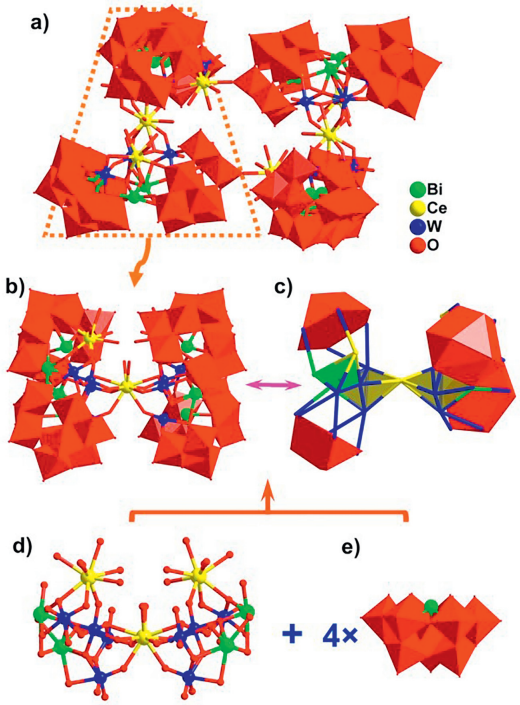

Fig. 1. (a) The ball-and-stick/polyhedral view of polyoxoanion **1a**. (b) Tetrameric **1b**. (c) Simplified view of **1b**. (d) Heterometallic cluster core $\{Ce_3W_8Bi_4\}$. (e) The BiW_9O_{33} fragment. Color codes: WO_6, red; W atom, blue; Ce atom, yellow; Bi atom, green; oxygen, red.

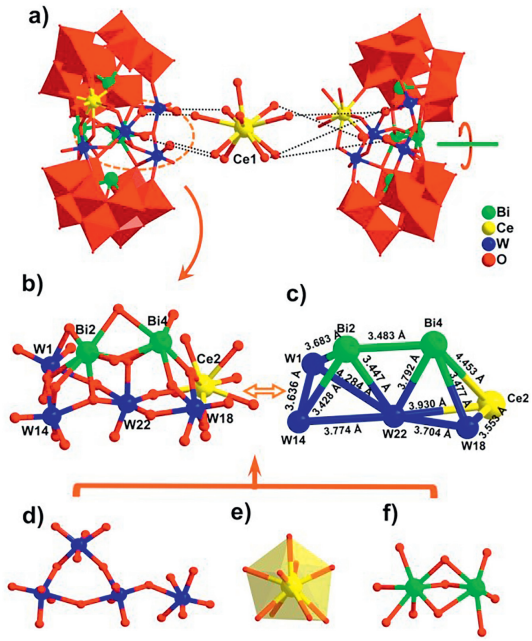

Fig. 2. (a) Connection mode between two dimeric **1c** and the Ce1 atom. (b) $\{CeW_4Bi_2\}$ cluster. (c) Distribution of the metal centers 4 W, 2 Bi and 1 Ce. (d) $\{W_4\}$ cluster. (e) The nine-coordinated geometry of Ce2. (f) $\{Bi_2\}$ cluster.

La^{3+}, Pr^{3+}, Nd^{3+}) [42], and a giant aggregate $\{[W_{14}Ce^{IV}{}_6O_{61}]([W_3Bi_6Ce^{III}{}_3(H_2O)_3O_{14}][BiW_9O_{33}]_3)_2\}^{34-}$ with high proton conductivity [43]. As a result, the construction of novel Bi-based Ln-POMs, although still highly challenging, has attracted our great interest and provided a huge opportunity for further exploration.

In this study, the one-pot reaction of $Na_2WO_4{\cdot}2H_2O$, $Ce(NO_3)_3{\cdot}6H_2O$, $Bi(NO_3)_3{\cdot}5H_2O$ resulted in the isolation of a novel one-dimensional chain architecture established by Ce-containing tungstobismuthate aggregate $Cs_{18}Na_8H_{20}[Ce_3(H_2O)_{10}W_8Bi_4O_{28}(B\text{-}\alpha\text{-}BiW_9O_{33})_4]_2{\cdot}64H_2O$ (**1**), which was systematacially characterized by the powder X-ray diffraction, infrared spectroscopy and thermogravimetric analysis (Figs. S1-S3 in Supporting information). To the best of our knowledge, **1** is the first reported Ln-POM with an extended structure based on tungstobismuthate building blocks, enriching the structural diversity of POM family. From the perspective of structure assembly, the formation of title compound **1** is mainly dependent on the powerful structure-directing effect of trigonal pyramidal heteroatoms, as well as the high oxygen affinity of Ln species. Specifically, lone-paired electrons located on top of the trigonal pyramidal Bi atoms directed toward the opening of the $\{BiW_9\}$ fragments, which effectively prevents the clusters assembling into a saturated POM building units. The high coordination number, long bond and large radius of Ce atoms at hinge sites play crucial roles in connecting POM fragments to form huge aggregate and further constructing extended structure. Additionally, catalytic experiments indicate that **1**, as a heterogeneous catalyst, has the ability to efficiently and selectively oxidize CEES into the nontoxic sulfoxide product CEESO, and could be reused five times while maintaining its high catalytic activity.

Single-crystal X-ray diffraction reveals that compound **1** crystallizes in the monoclinic system C2/*c* space group (Table S1 in Supporting information). The molecular structural unit is composed of 18 Cs^+, 8 Na^+, 20 H^+ and an unprecedented octameric polyoxoanion $[Ce_3(H_2O)_{10}W_8Bi_4O_{28}(B\text{-}\alpha\text{-}BiW_9O_{33})_4]_2^{46-}$ (**1a**, Fig. 1a) composed of two tetrameric entities $[Ce_3(H_2O)_{10}W_8Bi_4O_{28}(B\text{-}\alpha\text{-}BiW_9O_{33})_4]^{23-}$ (**1b**, Figs. 1b and c) linked by two Ce–O–W bonds. Bond valence sum (BVS) [44] calculations indicate that all the Ce, Bi and W atoms are in the formal +3, +3 and +6 oxidation states, respectively. And all terminal oxygens (O16/59/67/73/85) on Ce atoms are coordination water molecules as determined by corresponding BVS values (Table S2 in Supporting information). Each **1b** contains a heterometallic cluster core $Ce_3(H_2O)_{10}W_8Bi_4O_{28}$ ($\{Ce_3W_8Bi_4\}$) ligated by four $B\text{-}\alpha\text{-}BiW_9O_{33}$ ($\{BiW_9\}$) fragments through the Ce–O–W, W–O–W and Bi–O–W linkages (Figs. 1d and e). As shown in Fig. 2a, **1b** can be also structurally viewed as fusion of two dimeric subunits $[Ce(H_2O)_4W_4Bi_2O_{14}(B\text{-}\alpha\text{-}BiW_9O_{33})_2]^{13-}$ (**1c**) by virtue of a central Ce1 atom, and two **1c** are nearly perpendicular to each other. The bridging Ce1 is ten-coordinated with a di-capped tetragonal antiprism geometry, which is bonded to eight oxygen atoms from two **1c** on both sides and the residual two coordination sites are occupied by terminal water ligands [Ce–O: 2.473(8)–2.819(8) Å].

Each **1c** is constructed from two $\{BiW_9\}$ fragments sandwiching a $Ce(H_2O)_4W_4Bi_2O_{14}$ ($\{CeW_4Bi_2\}$) cluster core. The $\{BiW_9\}$ fragments are *in-situ* generated by using $Na_2WO_4{\cdot}2H_2O$ as starting materials combined with the Bi heteroatom templates, which play an important structure-directing role in the construction of polynuclear metal centers. The $\{CeW_4Bi_2\}$ cluster contains 4 W, 2 Bi and 1 Ce atoms, and interestingly, these metal centers exactly constitute a pair of virtual distorted tetrahedrons arranged side by side through a common W22 atom, with W···W distances of 3.636–4.284 Å, W···Ce distances of 3.553–3.930 Å and W···Bi distances of 3.428–3.792 Å (Figs. 2b and c). In the heterometallic $\{CeW_4Bi_2\}$ cluster, four crystallographically independent W centers are all six-coordinated octahedron geometry with the W–O bond lengths in the range of 1.721(9)–2.321(8) Å, three (W1, W14 and W22) of which are edge-shared to each other forming a $\{W_3\}$ triad, further connecting the W18 in a vertex-sharing fashion to form the unique $\{W_4\}$ cluster (Fig. 2d). Bi2 and Bi4 atoms are connected to each other in a coplanar manner forming a Bi_2O_{10} ($\{Bi_2\}$) cluster (Fig. 2f) with Bi–O bond lengths in the range of 2.166(8)–2.621(8) Å, which are quite different from the Bi1 and Bi3 atoms that act as

primary heteroatoms coordinated with three oxygen atoms forming BiO_3 trigonal pyramids with the Bi–O bond lengths varying from 2.130(8) Å to 2.167(10) Å in the center of $\{BiW_9\}$ fragments. The coordination environment of $\{Bi_2\}$ cluster is completed by four oxygen atoms from the $\{W_4\}$ cluster and six oxygen atoms from two $\{BiW_9\}$ fragments. Ce2 adopts the mono-capped tetragonal antiprism geometry (Fig. 2e) coordinated by one oxygen atoms from the vacant position of one $\{BiW_9\}$ fragment, one terminal oxygen atom from another $\{BiW_9\}$ fragment, three oxygen atoms from the $\{CeW_4Bi_2\}$ cluster and four terminal water ligands, with the Ce–O bond lengths falling in the range of 2.374(8)–2.646(9) Å.

Furthermore, it should be noted that Ce2 atoms also serve as bridges to link adjacent **1a** together through the Ce–O–W bonds, generating infinitely 1D chain, which reveals a new type of octameric Ln-POM cluster with extended structure based on the tungstobismuthate building blocks. And the 1D chains are aligned in an –ABAB– mode in the *ab* plane (Fig. S5 in Supporting information).

Sulfur mustard (also known as mustard gas or HD), one of the most notorious chemical warfare agents, was first used in World War I, which can cause painful skin blisters, serious irritation to eyes and respiratory system, damage to DNA, and even death at high doses [45–49]. Continued use and demand for stockpile destruction prompt research into the development of efficient materials to safely handle sulfur mustard. The partial oxidation of sulfur mustard to the nontoxic sulfoxide product is one of the most favorable decontamination pathways [50–52]. To achieve this goal, various catalyst materials have been developed and estimated for the selective oxidation of a sulfur mustard simulant CEES to the nontoxic CEESO [53–55]. POMs exhibit great potential for the detoxification of CEES due to their tunability, multifunctionality and high stability, especially in the reaction system using H_2O_2 as an oxidant [56–61].

Herein, the catalytic oxidative experiments for CEES were carried out in methanol (4 mL) solvent with compound **1** as the catalyst (0.5 μmol) and 30% H_2O_2 as the oxidant (0.55 mmol) under ambient temperature (*ca.* 30 °C), and the reaction process was monitored by gas chromatography-flame ionization detector (GC-FID). In the presence of H_2O_2 alone without catalyst (blank test), CEES was oxidized at a conversion rate of 36% in 35 min, (Fig. S6 in Supporting information). As shown in Fig. 3, compound **1** displayed excellent catalytic effect on the oxidation of CEES. The residual content of CEES in the reaction system decreased with reaction time, and the conversion reached 98% within 35 min in the presence of **1**. More importantly, high selectivity of 96% for CEESO was achieved. In addition, the kinetics of CEES oxidation reaction was investigated according to the conversion rates changing as a function of time. The $\ln(C_t/C_0)$ is correlated linearly with the reaction time, revealing that the oxidation process of CEES is in conformity with pseudo first-order dynamic equation with a rate constant k_1 of 0.11632 min^{-1} and a half-life of approximately 6 min (Fig. S7 in Supporting information). Further, as a heterogeneous catalyst, **1** can be easily recovered by filtration, and then reused in a new reaction batch. Fig. 4 showed that there was no significant loss of catalytic activity of the recovered **1** and CEES was high-selectively oxidized to the CEESO in five successive cycles, indicating the steady reusability of compound **1** (Fig. S8 in Supporting Information). IR and PXRD of the recycled catalyst matched well with those of the pristine **1** (Figs. S9 and S10 in Supporting information), confirming that compound **1** retained its structural integrity after the catalytic oxidation reaction.

In summary, a new Ce-containing tungstobismuthate has been prepared under conventional aqueous solution conditions. Its octameric polyoxoanion is composed of two tetrameric half-units $[Ce_3(H_2O)_{10}W_8Bi_4O_{28}(B\text{-}\alpha\text{-}BiW_9O_{33})_4]^{23-}$ connected by the Ce–O–W bonds, and further bridged by Ce linkers to form infinitely

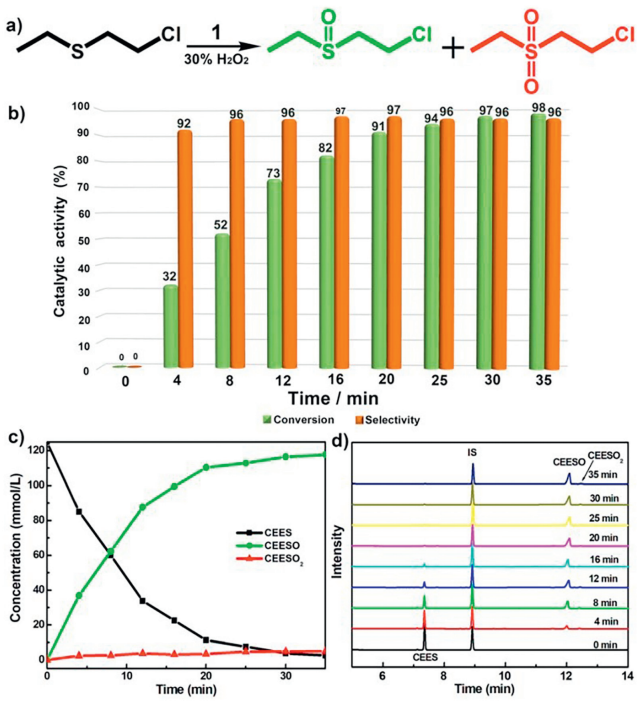

Fig. 3. (a) Oxidative abatement of CEES by **1** using 30% H_2O_2. (b) Conversion of CEES and selectivity of CEESO with catalyst **1**. (c) Plots of the CEES decontamination over reaction time by using catalyst **1**. (d) GC-FID signals for the catalytic process. Internal standard: 0.25 mmol dichlorobenzene; CEES: 0.50 mmol).

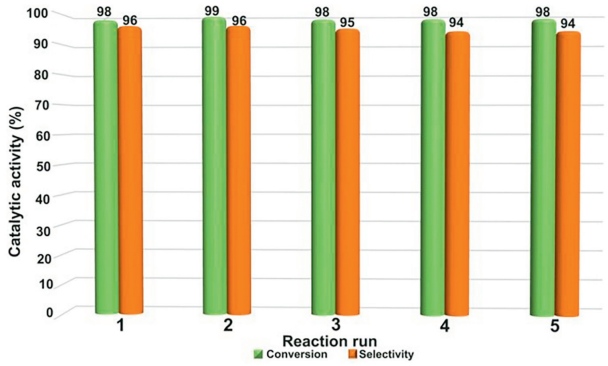

Fig. 4. Recycle tests of catalyst **1** in the oxidative decontamination of CEES.

1D chain. Such a Ln-POM with extended structure based on the tungstobismuthate building blocks is observed for the first time. The structure-directing effect of trigonal pyramidal heteroatom and high oxygen affinity of Ln species play crucial roles in the construction of large aggregate. Additionally, as a recyclable heterogeneous catalyst, **1** demonstrates high catalytic activity and selectivity for the oxidation degradation of CEES into CEESO. Continuous research of the assembly of novel Ln-based tungstobismuthate clusters with multifunctionality is currently in progress.

Declaration of competing interest

The authors declare that there are no conflicts of interest.

Acknowledgments

The authors gratefully acknowledge the financial support from the National Natural Science Foundation of China (No. U1704164), the Basic Research Project of Henan Provincial Key Scientific Research Project (No. 22ZX002).

Supplementary materials

Supplementary material associated with this article can be found, in the online version, at doi:10.1016/j.cclet.2023.109343.

References

[1] S.T. Zheng, G.Y. Yang, Chem. Soc. Rev. 41 (2012) 7623–7646.
[2] J. Lin, N. Li, S. Yang, et al., J. Am. Chem. Soc. 142 (2020) 13982–13988.
[3] D.L. Long, R. Tsunashima, L. Cronin, Angew. Chem. Int. Ed. 49 (2010) 1736–1758.
[4] H.L. Li, M. Zhang, C. Lian, et al., CCS Chem. 2 (2020) 2095–2103.
[5] Y.L. Wu, X.X. Li, Y.J. Qi, et al., Angew. Chem. Int. Ed. 57 (2018) 8572–8576.
[6] S.R. Li, H.Y. Wang, H.F. Su, et al., Small Methods 5 (2021) 2000777.
[7] S.S. Wang, G.Y. Yang, Chem. Rev. 115 (2015) 4893–4962.
[8] J. Liu, W. Shi, X. Wang, J. Am. Chem. Soc. 143 (2021) 16217–16225.
[9] K. Qin, D. Zang, Y. Wei, Chin. Chem. Lett. 34 (2023) 107999.
[10] K. Zheng, B. Niu, C. Lin, et al., Chin. Chem. Lett. 34 (2023) 107238.
[11] Q. Zhang, F.Y. Li, L. Xu, Polyoxometalates 2 (2023) 9140018.
[12] H.L. Li, C. Lian, D.P. Yin, et al., Inorg. Chem. 59 (2020) 12842–12849.
[13] J.X. Liu, N.V. Izarova, P. Kögerler, Chem. Commun. 55 (2019) 10744–10747.
[14] X. Xu, Y. Chen, Y. Zhang, et al., Inorg. Chem. 58 (2019) 11636–11648.
[15] Y. Ma, F. Gao, W. Xiao, et al., Chin. Chem. Lett. 33 (2022) 4395–4399.
[16] Z. Li, X.X. Li, T. Yang, et al., Angew. Chem. Int. Ed. 56 (2017) 2664–2669.
[17] Y.N. Gu, Y. Chen, Y.L. Wu, et al., Inorg. Chem. 57 (2018) 2472–2479.
[18] S. Li, Z. Weng, L. Jiang, et al., Chin. Chem. Lett. 34 (2023) 107251.
[19] J. Goura, B.S. Bassil, J.K. Bindra, et al., Chem. Eur. J. 26 (2020) 15821–15824.
[20] X.B. Han, Z.M. Zhang, T. Zhang, et al., J. Am. Chem. Soc. 136 (2014) 5359–5366.
[21] Z.M. Zhang, X. Duan, S. Yao, et al., Chem. Sci. 7 (2016) 4220–4229.
[22] Z.M. Zhang, S. Yao, Y.G. Li, et al., Chem. Commun. 49 (2013) 2515–2517.
[23] J. Cai, X.Y. Zheng, J. Xie, et al., Inorg. Chem. 56 (2017) 8439–8445.
[24] Y.J. Wang, S.Y. Wu, Y.Q. Sun, et al., Chem. Commun. 55 (2019) 2857–2860.
[25] D. Wang, J. Jiang, M.Y. Cao, et al., Nano Res. 15 (2022) 3628–3637.
[26] L. Liu, J. Jiang, L. Cui, et al., Inorg. Chem. 61 (2022) 1949–1960.
[27] Z. Li, Z.H. Lv, H. Yu, et al., CCS Chem. 4 (2022) 2938–2945.
[28] S.R. Li, W.D. Liu, L.S. Long, et al., Polyoxometalates 2 (2023) 9140022.
[29] S.X. Shang, Z.G. Lin, A.X. Yin, et al., Inorg. Chem. 57 (2018) 8831–8840.
[30] Z.K. Zhu, Y.Y. Lin, R.D. Lai, et al., Chin. Chem. Lett. 34 (2023) 107773.
[31] J.M. Cameron, J. Gao, D.L. Long, et al., Inorg. Chem. Front. 1 (2014) 178–185.
[32] I.V. Kalinina, E.V. Peresypkina, N.V. Izarova, et al., Inorg. Chem. 53 (2014) 2076–2082.
[33] E. Tanuhadi, N.I. Gumerova, A. Prado-Roller, et al., Inorg. Chem. 60 (2021) 8917–8923.
[34] J. Li, N. Song, M. Wang, et al., Inorg. Chem. 61 (2022) 17166–17177.
[35] J.W. Zhao, H.L. Li, X. Ma, et al., Sci. Rep. 6 (2016) 26406.
[36] K. Wassermann, M.H. Dickman, M.T. Pope, Angew. Chem. Int. Ed. 36 (1997) 1445–1448.
[37] K. Fukaya, T. Yamase, Angew. Chem. Int. Ed. 42 (2003) 654–658.
[38] W.C. Chen, H.L. Li, X.L. Wang, et al., Chem. Eur. J. 19 (2013) 11007–11015.
[39] W.C. Chen, C. Qin, X.L. Wang, et al., Dalton Trans. 44 (2015) 11290–11293.
[40] H.L. Li, C. Lian, L.J. Chen, et al., Nanoscale 12 (2020) 16091–16101.
[41] H.L. Li, C. Lian, L.J. Chen, et al., Inorg. Chem. 58 (2019) 8442–8450.
[42] K. Cui, F. Li, L. Xu, et al., Dalton Trans. 41 (2012) 4871–4877.
[43] J.C. Liu, Q. Han, L.J. Chen, et al., Angew. Chem. Int. Ed. 57 (2018) 8416–8420.
[44] I.D. Brown, D. Altermatt, Acta Crystallogr. Sect. B: Struct. Sci. B41 (1985) 244–247.
[45] A. Atilgan, T. Islamoglu, A.J. Howarth, et al., ACS Appl. Mater. Interfaces 9 (2017) 24555–24560.
[46] N. Emmanuel, P. Bianchi, J. Legros, et al., Green Chem. 22 (2020) 4105–4115.
[47] E. Oheix, E. Gravel, E. Doris, Chem. Eur. J. 27 (2021) 54–68.
[48] B.M. Smith, Chem. Soc. Rev. 37 (2008) 470–478.
[49] H.R. Tian, Z. Zhang, S.M. Liu, et al., J. Mater. Chem. A 8 (2020) 12398–12405.
[50] H. Wang, G.W. Wagner, A.X. Lu, et al., ACS Appl. Mater. Interfaces 10 (2018) 18771–18777.
[51] J. Dong, J. Hu, Y. Chi, et al., Angew. Chem. Int. Ed. 56 (2017) 4473–4477.
[52] F. Carniato, C. Bisio, R. Psaro, et al., Angew. Chem. Int. Ed. 53 (2014) 10095–10098.
[53] K. Ma, T. Islamoglu, Z. Chen, et al., J. Am. Chem. Soc. 141 (2019) 15626–15633.
[54] C.T. Buru, P. Li, B.L. Mehdi, et al., Chem. Mater. 29 (2017) 5174–5181.
[55] Y. Zhi, Z. Yao, W. Jiang, et al., ACS Appl. Mater. Interfaces 11 (2019) 37578–37585.
[56] N. Zhen, J. Dong, Z. Lin, et al., Chem. Commun. 56 (2020) 13967–13970.
[57] H.L. Li, C. Lian, G.Y. Yang, Sci. China Chem. 65 (2022) 892–897.
[58] J.Y. Sun, Z.L. Wang, Z. Zhang, et al., Polyoxometalates 3 (2024) 9140039.
[59] Y. Hou, H. An, Y. Zhang, et al., ACS Catal. 8 (2018) 6062–6069.
[60] H.L. Li, C. Lian, G.Y. Yang, Dalton Trans. 52 (2023) 857–861.
[61] L. Yang, Z. Zhang, C. Zhang, et al., Inorg. Chem. Front. 9 (2022) 4824–4833.